Incorporating high acidity cation on Co-free $BiFeO_3$-based air electrodes for enhancing electrocatalytic activity and durability in reversible solid oxide cells

Shun Wang[a], Wen Jiang[a], Yifeng Zheng[b*]

[a] College of Ceramics, Wuxi Vocational Institute of Arts & Technology, No. 99 South Jingyi Road, Yixing, 214200, Jiangsu, China

[b] College of Materials Science and Engineering, Nanjing Tech University, No. 30 Puzhu Road(S), Nanjing, 211816, Jiangsu, China

[*] Corresponding author.
Email address: zhengyifeng@njtech.edu.cn (Y. Zheng)

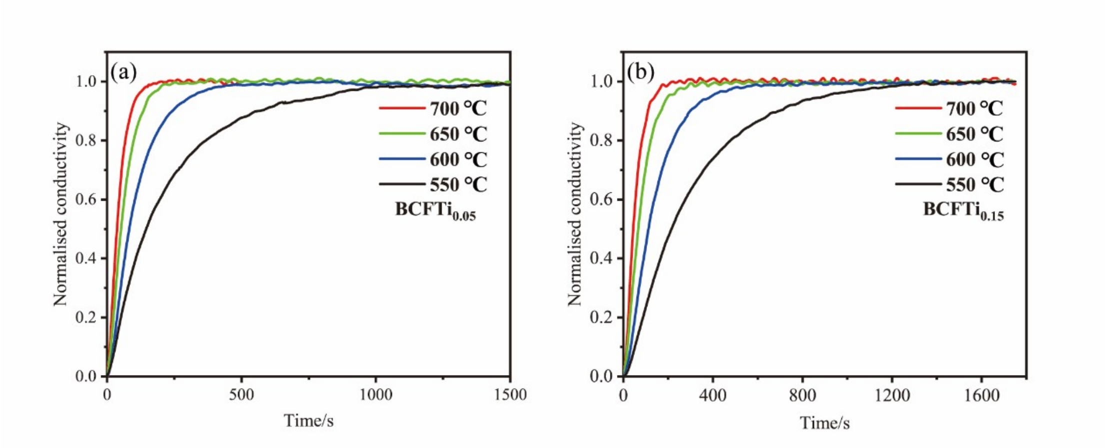

Fig.S1 ECR curves of (a)$BCFTi_{0.05}$ and (b) $BCFTi_{0.15}$ samples measured from 550 to 700 ℃ with an oxygen partial pressure changed from 0.1 to 0.21 atm.

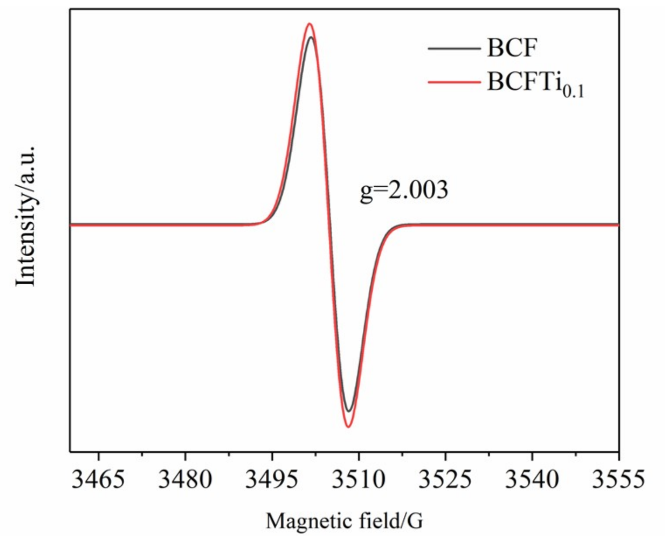

Fig. S2 EPR spectra of BCF and $BCFTi_{0.1}$ powders

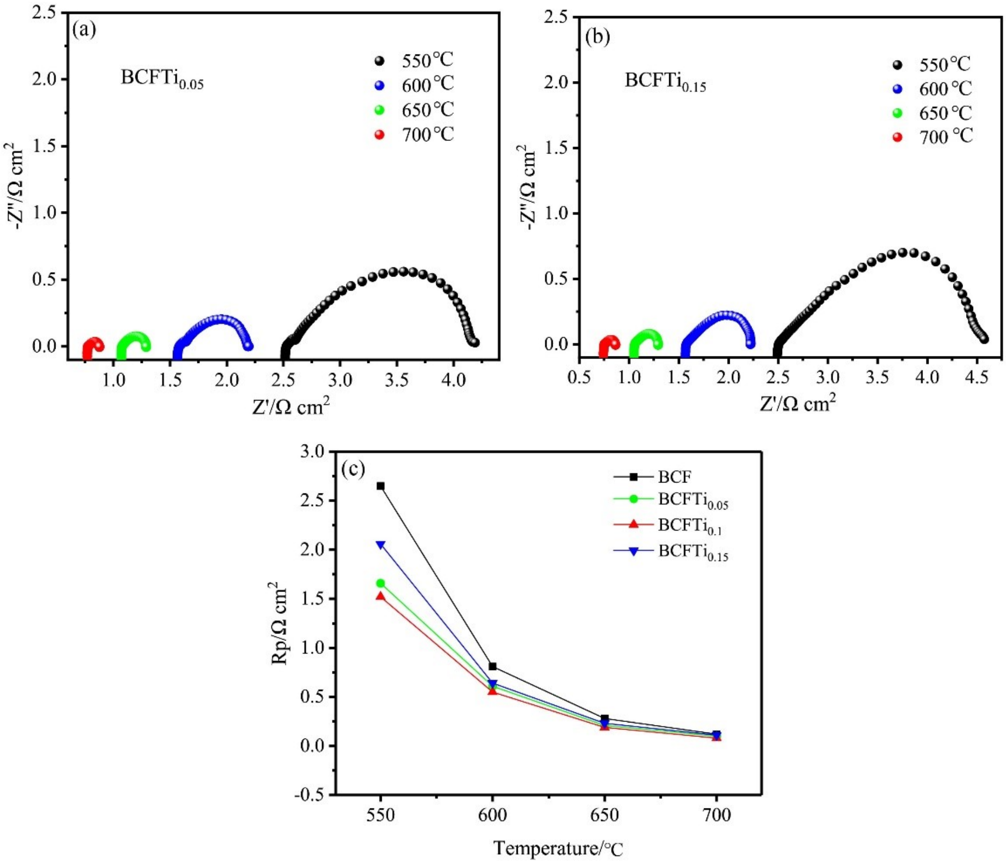

Fig.S3 EIS plots of (a) $BCF_{0.05}$ and (b) $BCFTi_{0.15}$ symmetrical cells measured at 550-700 ℃ in air; (c) The Rp values for BCFTix cathodes measured at 550-700 ℃ in air.

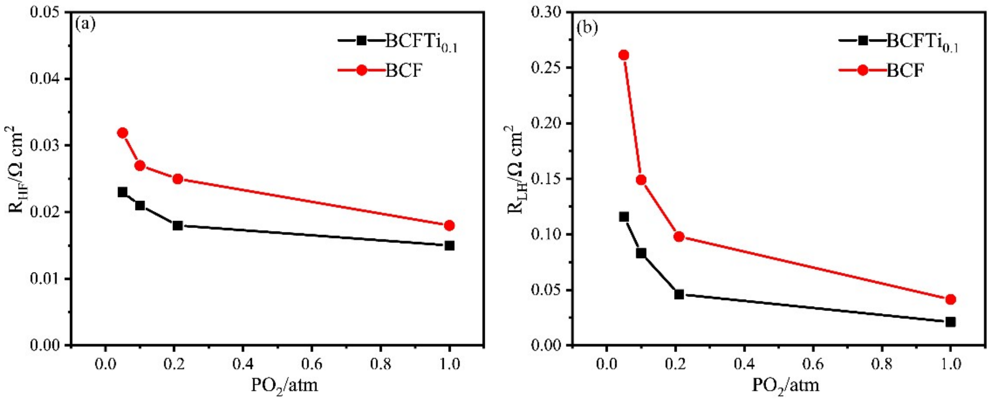

Fig.S4 (a)R_{HF} and (b)R_{LF} of BCF and $BCFTi_{0.1}$ cells on different pO_2 at 700 ℃.

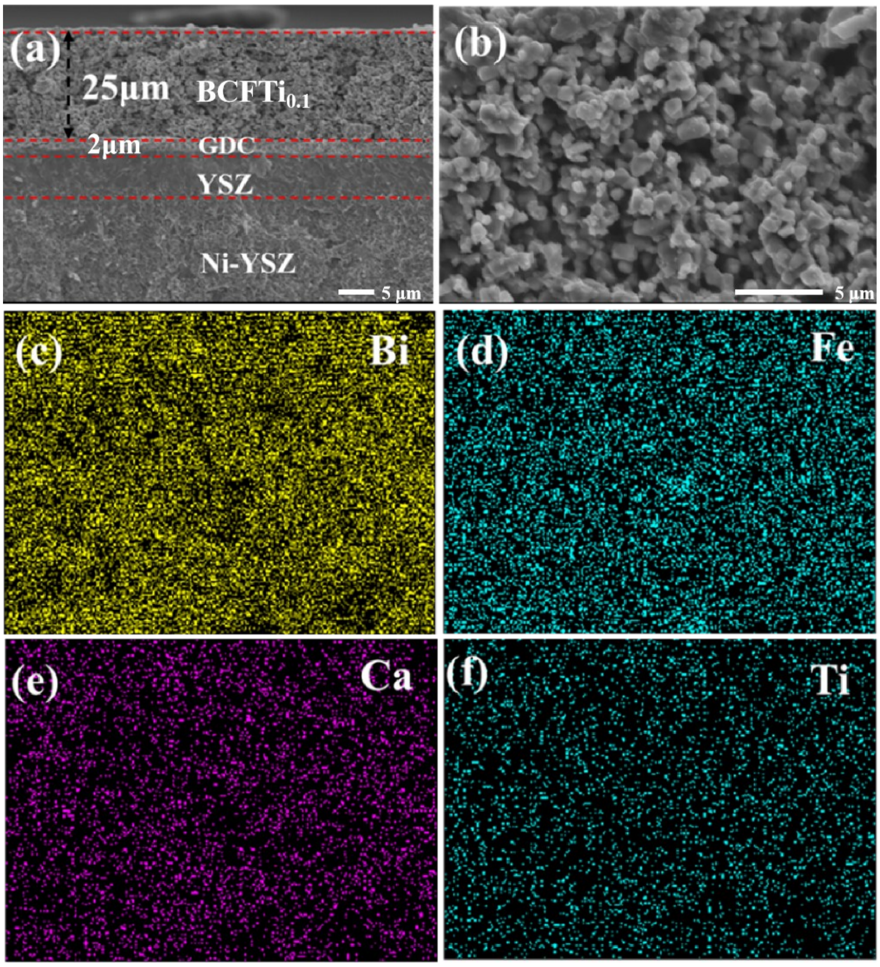

Fig. S5 SEM images of (a)Ni-YSZ/YSZ/GDC/BCFTi$_{0.1}$ single cell, (b) BCFTi$_{0.1}$ electrode surface morphology; EDS results of BCFTi$_{0.1}$ electrode (c) Bi, (d)Fe, (e)Ca and (f)Ti.

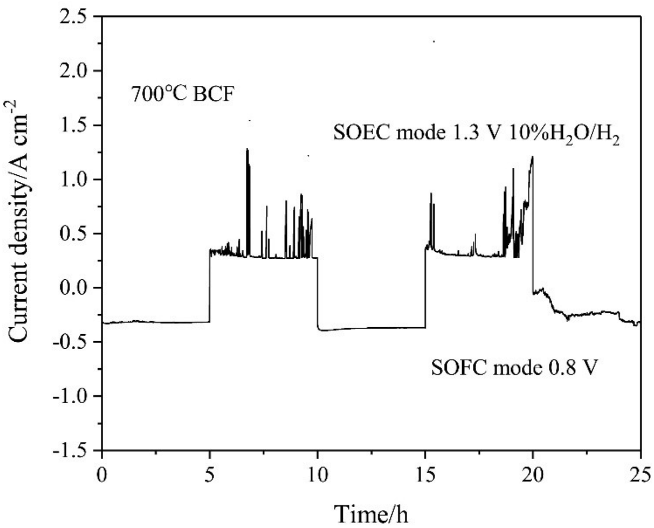

Fig.S6 Continuous cyclical operation between the SOFC mode (at 0.8 V) and the SOEC mode (at 1.3 V) at 700°C for BCF single cell.

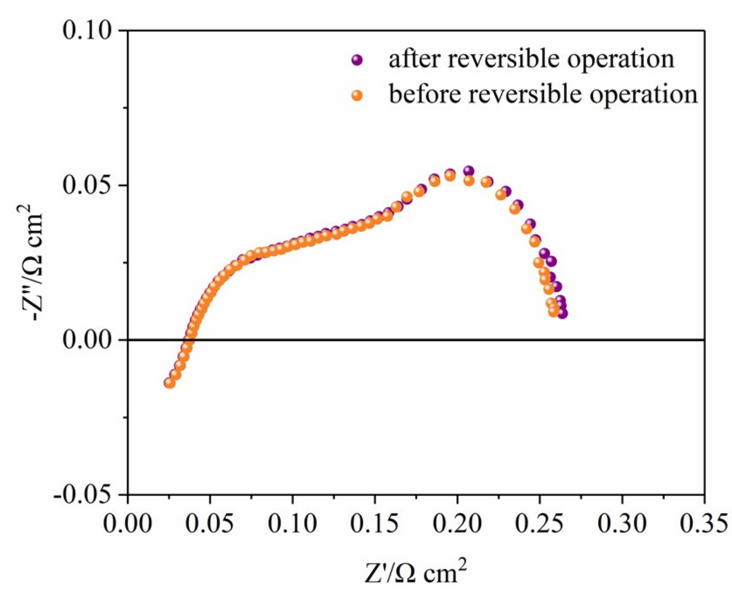

Fig. S7 EIS of the $BCFTi_{0.1}$ single cell before and after the continuous cyclical operation.

Table S1 Lattice parameters of $BCFTi_xO_{3-\delta}$ (x=0, 0.05, 0.1, 0.15) samples

Samples	Space group	a=b=c	ωRp	Rp	χ^2
BCF	Pm-3m	3.91689	8.14	5.23	4.56
$BCFTi_{0.05}$	Pm-3m	3.91365	4.21	2.33	2.83
$BCFTi_{0.1}$	Pm-3m	3.92097	7.82	5.63	3.08
$BCFTi_{0.15}$	Pm-3m	3.92724	6.89	3.44	3.47

Table S2 Comparison of the Rp values of symmetrical cells with various Fe-based or Co-based perovskite materials measured at 700 ℃ in air

Cathode	Electrolyte (μm)	Rp values (Ω cm^2)	Reference
$BCFTi_{0.1}$	GDC(~500)	0.064	This work
$Pr_{0.2}Ba_{0.2}Sr_{0.2}La_{0.2}Ca_{0.2}CoO_{3-\delta}$	LSGM (250)	~0.08	1
$Sr_{0.5}Bi_{0.5}FeO_{3-\delta}$	GDC(300)	~0.25	2
$Sr_{0.5}Bi_{0.4}Ca_{0.1}FeO_{3-\delta}$	GDC(300)	0.13	2
$Bi_{0.5}Sr_{0.5}Fe_{0.85}Ti_{0.15}O_{3-\delta}$	GDC(~300)	0.085	3
$Sm_2Ba_3Co_2Fe_3O_{15-\delta}$	LSGM (~280)	0.06	4
$SmBaCo_{0.8}Fe_{1.2}O_{5+\delta}$	LSGM (~280)	0.108	4
$SrCo_{0.8}Ti_{0.2}O_{3-\delta}$	LSGM(~200)	~0.062	5
$Bi_{0.5}Sr_{0.5}FeO_{3-\delta}$-$Ce_{0.9}Gd_{0.1}O_{1.95}$(7:3)	GDC(300)	0.14	6
$(La_{0.6}Sr_{0.4})_{0.95}Co_{0.2}Fe_{0.8}O_{3-\delta}$	LSGM (250)	0.091	7
$SmBaFe_2O_{5+\delta}$	LSGM (~270)	0.154	8

Table S3 Comparison in electrochemical performance (FC and EC mode) of $BCFTi_{0.1}$ single cell with reported high-performance cells using Co-based or Fe-based air electrodes

Air Electrode	Fuel electrode/electrolyte	MPD (W cm^{-2})	Current density (A cm^{-2})	Reference
$BCFTi_{0.1}$	Ni-YSZ/YSZ/GDC	1.03 (700 °C)	0.9 (700 °C, 70 H_2O:30 H_2, 1.3V)	This work
PCFC	Ni-YSZ/YSZ/GDC	0.493 (700 °C)	0.79 (750 °C, 50 H_2O:50 H_2, 1.3V)	[9]
LSFN-GDC	Ni-YSZ/YSZ/GDC	0.729 (750 °C)	0.53 (750 °C, 50 H_2O:50 H_2, 1.3V)	[10]
RP-LSCFNMC	NiO-3YSZ-8YSZ|NiO-8YSZ|8YSZ|GDC	0.8 (700 °C)	0.76 (700 °C, 60 H_2O:40 H_2, 1.3V)	[11]
RP-LSC	NiO-3YSZ-8YSZ|NiO-8YSZ|8YSZ|GDC	0.57 (700 °C)	0.65 (700 °C, 60 H_2O:40 H_2, 1.3V)	[11]
BSFTF10	Ni-YSZ/YSZ/GDC	0.497 (700 °C)	0.958 (700°C, 70 CO_2:30CO, 1.5V)	[12]
LSFN	Ni-YSZ/YSZ/GDC	0.4 (700 °C)	0.32 (700 °C, 50 CO_2:50 H_2, 1.3V)	[13]
LSCF−SNDC	Ni-YSZ/YSZ/SNDC	1.13 (700 °C)	1.37 (750 °C, 50 H_2O:50 H_2, 1.3V)	[14]
LBSNF-GDC	Ni-YSZ/YSZ/GDC	0.418 (700 °C)	0.36 (700 °C, 50 H_2O:50 H_2, 1.3V)	[15]
NCBC2	Ni-YSZ/YSZ/GDC	~0.8 (700 °C)	0.81 (800 °C, 70 CO_2:30H_2, 1.5V, single cell configuration: NCBC2/LSGM/SFM-SDC)	[16]

PCFC: $Pr_{0.8}Ca_{0.2}Fe_{0.8}Co_{0.2}O_{3-\delta}$; LSFN-GDC: $La_{0.6}Sr_{0.4}Fe_{0.8}Ni_{0.2}O_{3-\delta}$-$Gd_{0.1}Ce_{0.9}O_{2-\delta}$; RP-LSCFNMC: $La_{1.4}Sr_{0.6}Co_{0.2}Fe_{0.2}Ni_{0.2}Mn_{0.2}Cu_{0.2}O_{4\pm\delta}$; RP-LSC: $La_{1.4}Sr_{0.6}CoO_{4\pm\delta}$; BSFTF10： $Bi_{0.5}Sr_{0.5}Fe_{0.9}Ta_{0.1}O_{3-\delta}F_{0.1}$; LSFN: $La_{0.6}Sr_{0.4}Fe_{0.9}Nb_{0.1}O_{3-\delta}$; LSCF-SNDC: $La_{0.6}Sr_{0.4}Co_{0.2}Fe_{0.8}O_{3-\delta}$-$Sm_{0.075}Nd_{0.075}Ce_{0.85}O_{2-\delta}$; LBSNF-GDC: $La_{0.8-x}Bi_xSr_{0.2}Ni_{0.2}Fe_{0.8}O_{3-\delta}$- $Gd_{0.1}Ce_{0.9}O_{2-\delta}$; NCBC2: $Nd_{0.8}Ca_{0.2}BaCo_2O_{5+\delta}$; LSGM: $La_{0.9}Sr_{0.1}Ga_{0.8}Mg_{0.2}O_{3-\delta}$; SFM-SDC: $Sr_2Fe_{1.5}Mo_{0.5}O_{6-\delta}$-$Ce_{0.8}Sm_{0.2}O_{1.9}$.

Reference:

1 He, F.; Zhu, F.; Liu, D.; Zhou, Y.; Sasaki, K.; Choi, Y.; Liu, M.; Chen, Y. *Mater. Today*, 2023, **63**, 89-98.

2 Gao, J.; Liu, Y.; Xia, T.; Sun, L.; Zhao, H.; Wei, B.; Li, Q. *Sep. Purif. Technol.*, 2023, **311**, 123267.

3 Gao, J.; Li, Q.; Xia, W.; Sun, L.; Huo, L.-H.; Zhao, H. *ACS Sustainable Chem. Eng.*, 2019, **7**, 18647-18656.

4 Sun, Z.; Shen, Z.; Du, Z.; Zhang, Y.; Gong, Y.; Zhang, M.; Wang, K.; Świerczek, K.; Zeng, J.; Zhao, H. *Adv. Funct. Mater.*, 2024, **34**, 2403312.

5 Dang, X.; Li, T.; Jiang, Y.; Gao, Z.; Hua, Y.; Su, H. *J. Power Sources*, 2024, **603**, 234448.

6 Gao, J.; Li, Q.; Guo, M.; Sun, L.; Huo, L.; Zhao, H. *Ceram. Int.*, 2021, **47**, 748-754.

7 Zhu, F.; He, F.; Xu, K.; Chen, Y. *Sci. China Mater.*, 2022, **65**, 3043-3052.

8 Zhang, M.; Du, Z.; Sun, Z.; Zhao, H. *J. Mater. Chem. A*, 2023, **11**, 21645-21654.

9 Li, Y.; Tian, Y.; Li, J.; Pu, J.; Chi, B. *J. Power Sources*, 2022, **528**, 231202.

10 Tian, Y.; Wang, W.; Liu, Y.; Zhang, L.; Jia, L.; Yang, J.; Chi, B.; Pu, J.; Li, J. *ACS Appl. Energy Mater.*, 2019, **2**, 3297-3305.

11 Li, X.; Chen, T.; Wang, C.; Sun, N.; Zhang, G.; Zhou, Y.; Wang, M.; Zhu, J.; Xu, L.; Wang, S. *Adv. Funct. Mater.*, 2024, 2411216.

12 Ye, H.; Feng, Y.; Shan, P.; Qian, B.; Ge, L.; Chen, H.; Zheng, Y. *Chem. Eng. J.*, 2024, **499**, 156105.

13 Guan, C.; Wang, Y.; Chen, K.; Xiao, G.; Lin, X.; Zhou, J.; Song, S.; Wang, J.-Q.; Zhu, Z.; Zhou, X.-D. *Mater. Lett.*, 2019, **245**, 114-117.

14 Park, J.H.; Jung, C.H.; Kim, K.J.; Kim, D.; Shin, H.R.; Hong, J.-E.; Lee, K.T. *ACS Appl. Mater. Interfaces*, 2021, **13**, 2496-2506.

15 Zheng, G.; Zhang, G.; Liu, K.; Huang, Z.; Chen, T.; Zhou, J.; Wang, S. *Int. J. Hydrogen Energy*, 2023, **48**, 12571-12580.

16 Li, J.; Sun, N.; Liu, X.; Shen, Y.; Wang, F.; Li, J.; Shi, K.; Jin, F. *J. Alloys Compd.*, 2022, **913**, 165245.